19th Australasian Fluid Mechanics Conference
Melbourne, Australia
8-11 December 2014

Experimental and Computational Analysis of a Typical Arterio-Venous Fistula

N. Lwin, M. Wahab, J. Carroll and T. Barber

School of Mechanical and Manufacturing Engineering
University of New South Wales, New South Wales 2052, Australia

Abstract

End Stage Renal Disease (ESRD) is the final stage of kidney failure where the kidneys are no longer able to perform their regulatory functions. Haemodialysis is the primary form of treatment for ESRD. Treatment requires vascular access to the blood stream with a sufficient increase in blood flow rates for effective dialysis. This is often achieved through the surgical anastomosis between the radial artery and cephalic vein known as an arteriovenous fistula (AVF). Complications arise from this including stenosis and thrombosis. To gain insight and understanding of these complications, an idealised AVF geometry has been modelled in CFD and also studied experimentally using particle imaging velocimetry (PIV). Results obtained showed significant flow disturbances with abnormally high and low values of wall shear stress (WSS). Correlation of trends in these haemodynamic factors at sites prone to failure supports hypotheses suggesting low WSS is the key factor in triggering complications leading to access failure. Other trends such as WSS gradients and oscillations were noted; however these characteristics require further quantification for investigation.

Introduction

A patient requiring Haemodialysis usually undergoes treatment four to five times per week and each session lasts as long as four to five hours. Blood is filtered via an extracorporeal system essentially acting as an artificial kidney (haemodialyser/dialyser) making use of an AVF for vascular access. It is essential to have a flow rate of 350-400 ml/min to minimise access recirculation and ensure efficient haemodialysis [11]. The flow rate within the radial artery normally is approximately 20-30 ml/min. With the complex geometric nature of an AV anastomosis, blood flow with relatively high Reynolds characteristics can be found causing turbulent flow and there are regions of high WSS along the venous wall, with significant flow separation and recirculation [7]. In the United States, 14-17% of hospitalisations in dialysis patients were due to vascular access-related complications [6] and long-term failure of an AVF is linked to the development of intimal hyperplasia (IH). Exact causes are unclear, however, haemodynamic factors such as recirculation zones and turbulence promoting abnormal WSS distributions are believed to stimulate the development of IH. While high levels of WSS can directly damage the endothelium and induce vascular remodelling, regions of low WSS are also believed to promote IH due to the increase in platelet adhesion and aggregation.

Typically, blood pressure in a healthy artery is approximately 10,000 Pa [5]. In comparison, wall shear stress (WSS) results from the frictional force of the viscous drag of blood tangentially along the inner layer (endothelial cells) and physiological levels of WSS in a healthy artery are 1-7 Pa [10]. Typical levels of WSS in healthy veins tend to be lower, from 0.1-0.6 Pa [10]. Very high levels (>35 Pa [9]) have been shown to damage the endothelial cells within an hour. WSS is difficult to physically quantify in experimental studies and has been determined through using a simplified model such as Poiseuilles law [3]; this however only yields a rough estimation of the averaged WSS acting on the endothelial cells.

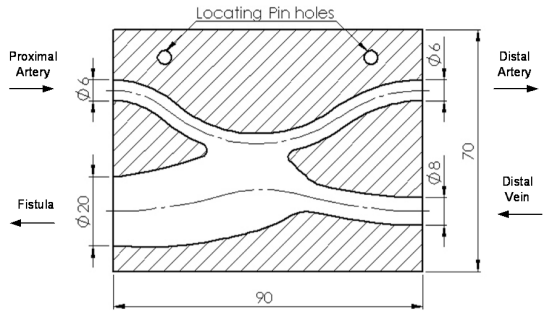

Figure 1: Experimental setup of AVF geometry, showing detail of AVF testpiece.

In this project, a computational and experimental study is conducted for an idealised AVF, to determine haemodynamic effects that may lead to vascular access failure. WSS, obtained from computational results, is used as a primary indicator.

Experimental validation

The experiment is conducted using an AVF machined from transparent modular acrylic blocks as shown in Figure 1. These modular pieces are placed on top of a groove in the aluminium base plate and the fistula block is located in the middle of the experimental rig. The fluid flows in from the arterial and flows out through the venous side. These blocks are connected together by 16 mm stainless steel dowel pins that ensure the blocks are in straight alignment. The design incorporates a side-to-side anastomosis and is scaled twice the actual size. Both the proximal artery and distal artery have the same diameter of 6 mm; the diameter of the proximal vein is 8 mm and the distal vein has the largest diameter of 20 mm.

Fluid flow into the rig is generated by a modified CardioFlow 1000MR pump, designed to generate realistic, accurate and repeatable physiological volume flow waveforms. The CardioFlow 1000MR has an accuracy of 1.0% and volume range of 0.1 to 35ml/s. In order to reduce light distortion, making the refraction index of the fluid to be the same with the acrylic block increases the accuracy of results. The composition of these fluid was approximately made from 53% sodium iodide (NaI), 30% water, and 16.3% glycerol. Sodium thiosulphate ($Na_2S_2O_3$) is added as well to prevent the fluid from becoming yellow, a natural process due to light exposure. This mixture has properties similar to blood at room temperature with a dynamic viscosity of 0.005384 Pa.s and density of 1692kg/m^3.

Particle Image Velocimetry (PIV) is used in this project to gain information about the AVF flow field. The system used is a Pegasus PIV, a product by New Wave Research (a division of Electro Scientific Industries, Inc). The Pegasus PIV utilizes a dual head, high repetition rate 527 nm Nd:YLF laser. Each laser head can be independently triggered and each laser pulse is uniform, having the same pulse width and same intensity. The laser beam projected beam diameter is 1.5mm and each laser head is

capable of operating up to 10,000 pulses per second and having frame rates up to 20,000 frames per second. The adaptive PIV method is used to iterative optimize the size and shape of each interrogation area in order to adapt to local flow gradients and seeding densities. Results were recorded at 400Hz with 180 image pairs used for each analysis.

Computational model

While RANS modelling is computationally efficient for many turbulent flow problems, to fully capture the oscillatory nature associated with pulsatile flow, a Large Eddy Simulation (LES) solution was used here. The filtered Navier Stokes equations are solved using a commercial finite volume code, Fluent, where the sub-grid-scale stresses are modelled using the dynamic Smagorinsky-Lilly model via the Boussinesq hypothesis [8]. In this model, Smagorinsky's eddy-viscosity formulation is used, however the square of the Smagorinsky constant is replaced by a coefficient. For a case of boundary layer flow, Geurts [4] finds that the dynamic model produces excellent accuracy with a significant saving of computational effort, when compared to DNS results. Momentum equations were solved by Central Differencing and Pressure-Velocity coupling was achieved with the PISO scheme. ICEM CFD within the ANSYS 14.5 software package was used to discretize the domain and a three-dimensional structured hexahedral mesh consisting of $3.2\text{x}10^6$ cells was created, as shown in Figure 2.

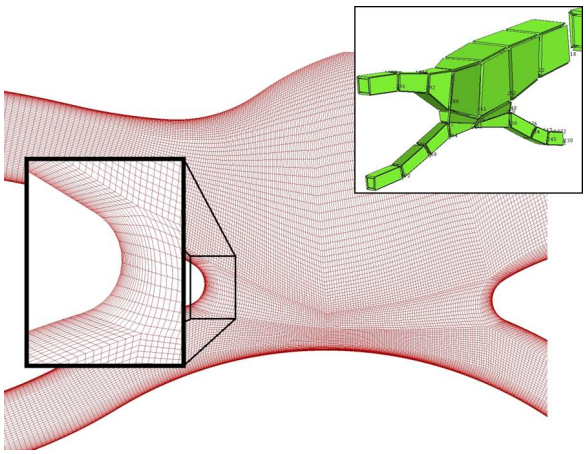

Figure 2: Mid plane view of refined mesh in the AVF region; inset shows ICEM blocking structure.

In addition to Reynolds number, characteristics of pulsatile flow are determined by Womersley number,

$$\alpha = R\sqrt{(\frac{\omega}{\nu})} \tag{1}$$

Where R = radius, ω = angular frequency of oscillation, ν = kinematic viscosity. A non-dimensional analysis was performed to scale the characteristic waveform to suit the sodium iodide and glycerol solution with the double scaled experimental rig, on the basis of both Reynolds and Womersley numbers. In doing so, the period of the waveform is increased to 1.066 s with maximum, minimum and mean centreline inlet velocities scaled to 0.499 m/s, 0.324 m/s and 0.387 m/s respectively. Limitations with the experimental pump exist, making pulsatile flow of such short periods unviable for concurrent experimental analysis. Hence, steady state flow with a constant velocity inlet is considered for the experimental comparisons. Haemodynamic analysis of subsequent transient computational results will be conducted at various points of interest across the pulsatile flow profile depicted below in Figure 3 (adapted from Remuzzi et al. [2]).

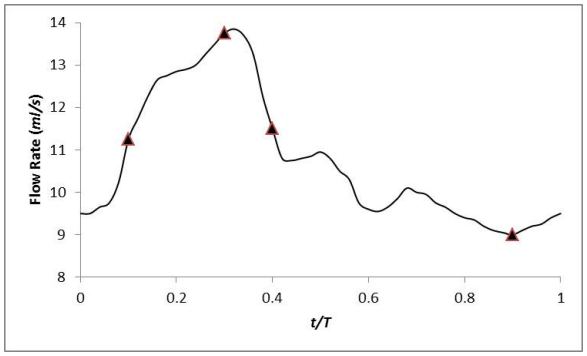

Figure 3: Points of interest on the characteristic pulsatile flow profile.

Results and Discussion

Initially, results were obtained for a number of (steady) flow rates, using PIV on the midplane of the AVF model. Figure 4 shows the results for 13 ml/s and 20 ml/s, and it can be seen that for both cases a large recirculating region is present in the middle of the targeted area. A high-speed region is found where the flow, entering from the proximal artery, turns into the fistula and speeds up along the wall. As is often the case physiologically, little flow was found in the distal segments.

Prior to full transient models being conducted, steady state comparisons between the experiment and the CFD simulations were made. Figure 5 shows the comparison for a position of X=40, for the two flowrates provided previously. The overall flow features are captured well, with the main discrepancy being the reverse flow peak at 20 ml/s. A possible source of this discrepancy lies in the PIV framerate not being sufficient to capture this range of velocity and further experimental work is being conducted to clarify this error.

Finally, transient (pulsatile) simulations were conducted, and results shown are from the fifth cardiac cycle simulated at the main points of interest. The main sites prone to develop haemodynamic complications are at the anastomosis site and the venous regions of the fistula [11]. Figure 6 shows the mid-plane velocity fields. Two distinct near wall stagnation points occur throughout the cardiac cycle. The first of which is at the toe of the anastomosis as the opposing flow of the feeding artery splits between the distal venous and arterial regions. This remains relatively constant in location and size. Conversely, the stagnation point at the upper venous wall appears to vary in size and location throughout the cardiac cycle where it is largest and most distal during systolic deceleration. Flow disturbances and the turbulent nature appear to be most pronounced during systolic deceleration, consistent with published studies [1].

Flow structures remain relatively consistent throughout with a significant recirculation zone in the core of the dilated vein of the fistula. There are recirculation zones present immediately distal from the fistula in both the vein and artery. The flow separation occurring in the arterial region immediately after the anastomosis is also observed in studies of end-to-side AVFs. The distal arterial flow is reversed with fluid returning towards the fistula. Disturbances in the draining vein seem to settle relatively quickly at systole; however, in diastole, another small recirculation appears as the vein straightens. This frequent change in near wall phenomena occurs in an area where thrombosis and stenosis are typically found [11] in clinical studies.

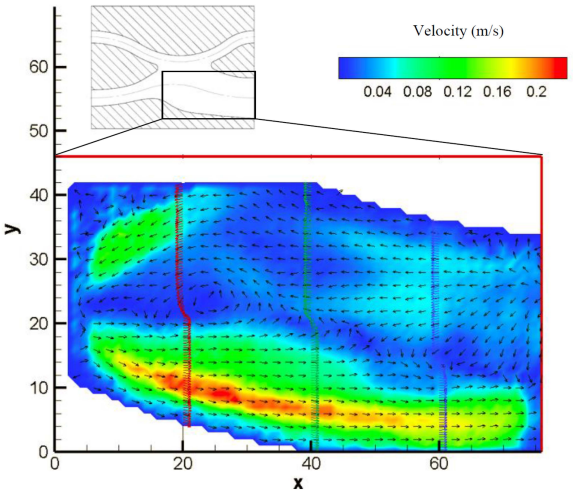

(a) 13 ml/s inlet velocity

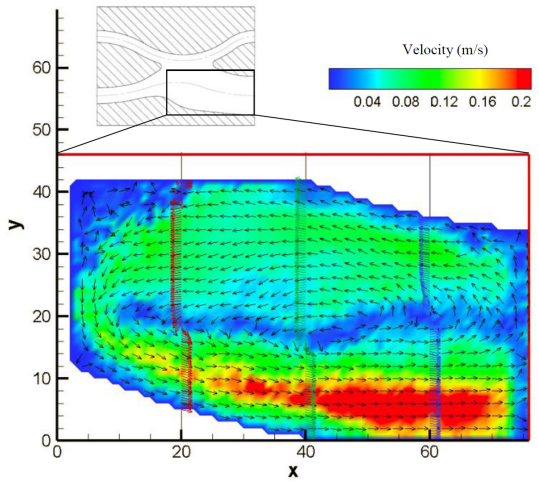

(b) 20 ml/s inlet velocity

Figure 4: Experimentally obtained contour and vector map for two flowrates (13 ml/s and 20 ml/s). Data-rate of 400hz, using 180 image pairs. X and Y are dimensionless locations.

Immediate flow separation occurs with the significant increase in cross sectional area across the AVF. Prominent regions of low flow exist centrally in the fistula as expected from the observed recirculation zone. Moderate to high flow is concentrated between the artery and the upper venous wall while near wall low flow remains either side of the fistula. The concentrated regions of near wall low flow may promote platelet adhesion and the observed formation of thrombosis. The disturbances caused by the toe of the anastomosis are made apparent with a slight development of a double vortex flow structure. While stenoses are found in this curved region of the vein, they were not considered to be progressive [11].

Literature has suggested WSS values of up to 7 Pa and as low as 1 Pa [10] to be physiological in a healthy human artery. Furthermore, typical venous WSS levels are observed to be approximately 0.76 Pa. In 7 the scale has been graded to highlight abnormal levels of WSS, where abnormally high regions are denoted as red on the contour and low regions are seen as a solid dark blue. WSS is believed to be one of the main factors in vascular remodelling. Significant regions of the dilated vein remain

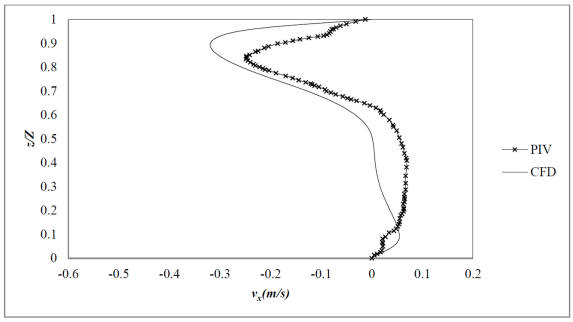

(a) 13 ml/s inlet velocity

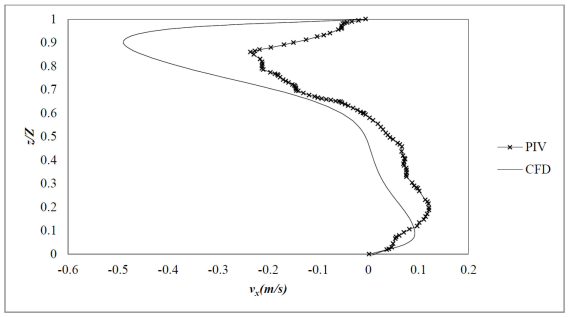

(b) 20 ml/s inlet velocity

Figure 5: Comparison of computational results with experimentally obtained data for two different flow rates, at a specified location as shown.

at abnormally low levels of WSS throughout the cardiac cycle. This venous region is also linked to IH development with stenosis and thrombosis commonly seen [11] supporting hypotheses that low WSS is a contributing factor. Low levels of WSS are also observed distally from the fistula. Even though this region is thought to be of little clinical significance, the distal vessels should still be monitored for the development of IH. It has to be noted, however, that this region has been simplified in this experimental model.

WSS levels remain within pathological range in the feeding artery prior to the curvature towards the anastomosis. At the curvature, however, the spatial WSS distribution observed creates a cause for concern. A region of abnormally low WSS is observed along the wall closest the anastomosis (attributed to the flow separation) in stark contrast to the significantly elevated WSS of up to 20.993 Pa during systole along the lower arterial wall. Significant WSS gradients such as this are observed to promote the production of vasodilators such as NO [10].

Similarly, WSS remains significantly elevated throughout the pulse around the toe while a sharp gradient is observed as low levels occur centrally at the near wall stagnation point. Maximum during systole is observed to be approximately 19 Pa, while in diastole, WSS is still abnormally high at approximately 10 Pa. Centrally at the stagnation point, however, WSS remains within physiological levels throughout. Given that the anastomosis site is generally linked to complications [11], this stipulates that WSS gradients may play a role in triggering the onset of IH. The temporal distribution of WSS varies significantly along the venous wall as the near wall stagnation point previously observed changes through the cardiac cycle. A large portion of the venous wall is seen to be above normal levels of WSS, reaching approximately 13 Pa during systole and systolic deceleration while the area is largely normal during diastole.

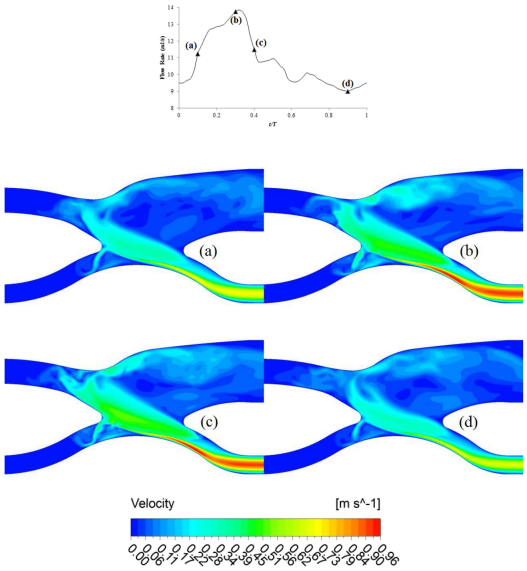

Figure 6: Mid-plane velocity contours at (a) t/T=0.1 (b) t/T=0.3 (c) t/T=0.4 (d) t/T=0.9.

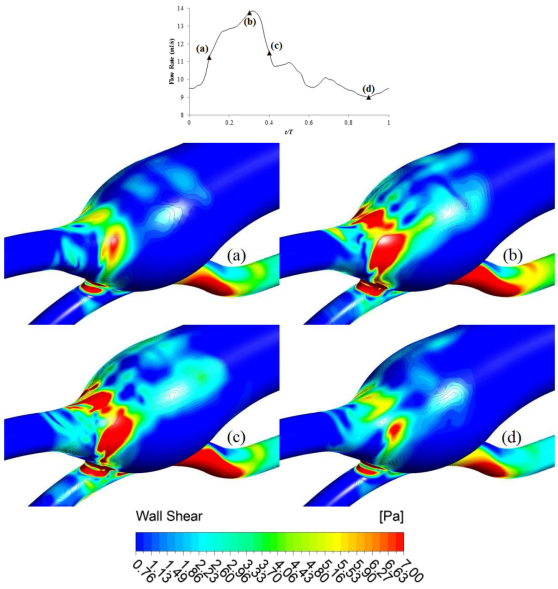

Figure 7: WSS contour plots of UNSW experimental rig during (a) t/T = 0.1 (b) t/T = 0.3 (c) t/T = 0.4 (d) t/T = 0.9.

Conclusions

Many complications result from the vascular access created in the form of an AVF. It is likely that stenosis and thrombosis form from the development of IH in regions of abnormally low WSS and disturbed flow. A CFD model was created and validated on the basis of steady state analysis of the double scaled UNSW AVF experimental rig. By incorporating CFD, we were able to overcome the associated physical limitations and gain insight on the flow conditions. An LES model was used to capture the full oscillatory nature of pulsatile flow and WSS. It was found that fluid accelerates through the feeding artery and is subject to significant flow disturbance across the anastomosis. A prominent recirculation zone was found in the venous region of the fistula with minimal flow occurring distally. Two key stagnation points were observed, one as flow division occurs at the toe and the other along the venous wall. Prominent regions of very low WSS were found, most significantly in the draining vein. This region has been highly correlated to failure subject to thrombosis and stenosis formation in clinical studies. This study supports hypotheses put forward in literature that low levels of WSS promote the development of IH. High levels of WSS were found in the feeding artery, toe and along the venous wall nearby the toe. These elevated levels of WSS will promote further dilation of the vessel in attempt to achieve homeostasis.

References

[1] Bessa, K. L. and Ortiz, J. P., Flow visualization in arteriovenous fistula and aneurysm using computational fluid dynamics, *Journal of visualization*, **12**, 2009, 95–107.

[2] Ene-Iordache, B., Mosconi, L., Remuzzi, G. and Remuzzi, A., Computational fluid dynamics of a vascular access case for hemodialysis, *Journal of biomechanical engineering*, **123**, 2001, 284–292.

[3] Ene-Iordache, B. and Remuzzi, A., Disturbed flow in radial-cephalic arteriovenous fistulae for haemodialysis: low and oscillating shear stress locates the sites of stenosis, *Nephrology Dialysis Transplantation*, **27**, 2012, 358–368.

[4] Geurts, B., Geurts, B. and Geurts, B., *Elements of direct and large-eddy simulation*, RT Edwards Philadelphia, PA, 2004.

[5] Hoskins, P. and Hardman, D., Three-dimensional imaging and computational modelling for estimation of wall stresses in arteries.

[6] Knoll, G. A., Wells, P. S., Young, D., Perkins, S. L., Pilkey, R. M., Clinch, J. J. and Rodger, M. A., Thrombophilia and the risk for hemodialysis vascular access thrombosis, *Journal of the American Society of Nephrology*, **16**, 2005, 1108–1114.

[7] Lee, S.-W., Smith, D. S., Loth, F., Fischer, P. F. and Bassiouny, H. S., Importance of flow division on transition to turbulence within an arteriovenous graft, *Journal of biomechanics*, **40**, 2007, 981–992.

[8] Lilly, D., A proposed modification of the germano subgrid-scale closure method, *Physics of Fluids*, **4**, 1992, 633–635.

[9] Niemann, A., Udesen, J., Thrysoe, S., Nygaard, J. V., Fründ, E., Petersen, S. E. and Hasenkam, J., Can sites prone to flow induced vascular complications in av fistulas be assessed using computational fluid dynamics?, *Journal of biomechanics*, **43**, 2010, 2002–2009.

[10] Papaioannou, T. G., Karatzis, E. N., Vavuranakis, M., Lekakis, J. P. and Stefanadis, C., Assessment of vascular wall shear stress and implications for atherosclerotic disease, *International journal of cardiology*, **113**, 2006, 12–18.

[11] Van Tricht, I., De Wachter, D., Tordoir, J. and Verdonck, P., Hemodynamics and complications encountered with arteriovenous fistulas and grafts as vascular access for hemodialysis: a review, *Annals of biomedical engineering*, **33**, 2005, 1142–1157.